Water Research 252 (2024) 121182

Contents lists available at ScienceDirect

Water Research

journal homepage: www.elsevier.com/locate/watres

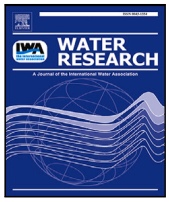

# Effect of vegetation treatment and water stress on evapotranspiration in bioretention systems

Simon De-Ville [a,*], Jill Edmondson [b], Daniel Green [c,d,1], Ross Stirling [c,d], Richard Dawson [c], Virginia Stovin [a]

[a] Department of Civil & Structural Engineering. The University of Sheffield, Sir Frederick Mappin Building, Mappin Street, Sheffield, South Yorkshire, S1 3JD, United Kingdom
[b] School of Biosciences. The University of Sheffield, Alfred Denny Building, Western Bank, Sheffield, South Yorkshire, S10 2TN, United Kingdom
[c] School of Engineering, Newcastle University, Newcastle-Upon-Tyne, NE1 7RU, United Kingdom
[d] UKCRIC National Green Infrastructure Facility, Newcastle-Upon-Tyne, NE4 5TG, United Kingdom

ARTICLE INFO

*Keywords:*
Evapotranspiration
Stormwater management
Urban green infrastructure
Bioretention
Hydrological performance
Sustainable Drainage Systems (SuDS)

ABSTRACT

Evapotranspiration is a key hydrological process for reducing stormwater runoff in bioretention systems, regardless of their physical configuration. Understanding the volumes of stormwater that can be returned to the atmosphere via evapotranspiration is, therefore, a key consideration in the design of any bioretention system. This study establishes the evapotranspiration dynamics of three common, structurally different, bioretention vegetation treatments (an Amenity Grass mix, and mono-cultures of *Deschampsia cespitosa* and *Iris sibirica*) compared with an un-vegetated control using lab-scale column experiments. Via continuous mass and moisture loss data, observed evapotranspiration rates were compared with those predicted by the FAO-56 Penman–Monteith model for five 14-day dry periods during Spring 2021, Summer 2021, and Spring 2022. Soil moisture reductions over the 14-day trials led to reduced rates of evapotranspiration. This necessitated the use of a soil moisture extraction function alongside a crop coefficient to represent actual evapotranspiration from FAO-56 Penman–Monteith reference evapotranspiration estimates. Crop coefficients ($K_c$) varied between 0.65 and 2.91, with a value of 1.0 identified as a recommended default value in the absence of treatment-specific empirical data. A continuous hydrological model with $K_c$ = 1.0 and a loading ratio of 10:1 showed that evapotranspiration could account for between 1 and 12% of the annual water budget for a bioretention system located in the UK and Ireland, increasing to a maximum of 35% when using the highest $K_c$ observed (2.91).

## 1. Introduction

### 1.1. Background

Evapotranspiration (ET), the combination of evaporation from exposed surfaces and transpiration from vegetation, can account for a significant portion of the annual water balance in undeveloped catchments. Across the UK, ET can account for 31 to 61% of the annual average water balance in Wales and southeastern England, respectively (Blyth et al., 2019). Traditionally, urban surface water management focused on removing rainfall as rapidly and efficiently as possible from urban surfaces to reduce the occurrence of urban flooding (Butler et al., 2018). These practices, combined with increased impermeable paved areas, result in the proportion of ET in an urban water balance being lower than in undeveloped environments. Blyth et al. (2019) highlight that mean ET rates in UK cities can be as much as 60% lower than their rural surroundings. However, the implementation of green infrastructure for stormwater management harnesses urban ET to reduce stormwater quantities while providing additional benefits, including Urban Heat Island reduction.

Green infrastructure designed for stormwater management is referred to globally under many different acronyms: SuDS—Sustainable Drainage Systems; LIDs—Low Impact Developments; GSI—Green Stormwater Infrastructure; or BMPs—Best Management Practices; amongst others (Fletcher et al., 2014). This article will henceforth refer to these devices as SuDS. Most vegetated SuDS primarily function in a similar way. Fig. 1 presents a generic process diagram for a vegetated bioretention device. Inflows are typically received at the system's surface, where there is ponding capacity to store stormwater volumes temporarily. The stormwater then infiltrates into the growing

* Correspondence to: Department of Civil and Environmental Engineering. University of Liverpool, The Quadrangle, Brownlow Hill, L69 3GH, United Kingdom.
*E-mail address:* simon.de-ville@liverpool.ac.uk (S. De-Ville).
[1] Present Address: School of Energy, Geoscience, Infrastructure and Society. Heriot-Watt University, Edinburgh, EH14 4AS, United Kingdom.

https://doi.org/10.1016/j.watres.2024.121182
Received 22 August 2023; Received in revised form 4 December 2023; Accepted 22 January 2024
Available online 24 January 2024
0043-1354/© 2024 The Author(s). Published by Elsevier Ltd. This is an open access article under the CC BY license (http://creativecommons.org/licenses/by/4.0/).

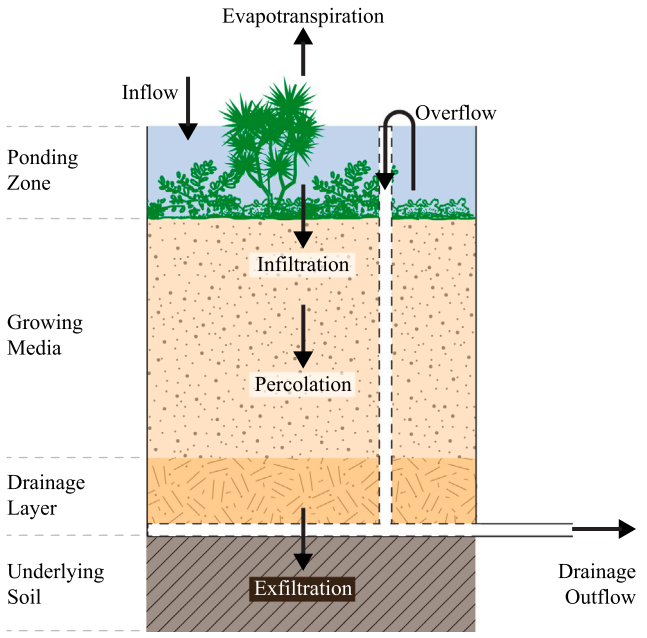


**Fig. 1.** Schematic diagram of an unlined bioretention system with underdrain. Key hydrological processes are also indicated (De-Ville et al., 2021).

media and percolates through it into a drainage/storage layer. Moisture retained within the growing media either evaporates back into the atmosphere or is actively removed from the growing media by plants and subsequently released back into the atmosphere by transpiration. Stormwater that collects in the drainage/storage layer may exfiltrate into underlying soils (provided the device is unlined) or drain via an underdrain which connects to downstream SuDS, a receiving water course or a sewer network.

### 1.2. Factors influencing ET rates

ET rates are predominantly a function of meteorological variables, vegetation characteristics, and soil moisture relationships[2] (Nasrollahpour et al., 2022). There are four key meteorological factors: solar radiation, air temperature, humidity, and wind speed (Allen et al., 1998). Vegetation type, growth stage, density and water use strategy have all been demonstrated to influence the rate of actual ET (Allen et al., 1998; Wadzuk et al., 2013; Berretta et al., 2014; Poë et al., 2015). Soil moisture levels are critical, as ET processes can only consume the finite volumes of water retained within the soil matrix. As moisture levels decrease below field capacity towards the vegetation wilting point, the matric potential of soil water increases, leading to a reduced extraction of soil water by plant roots and hence reduced rates of ET (Zhao et al., 2013).

### 1.3. Estimating ET from meteorological data

Estimates of theoretical ET values under well-watered conditions can be derived from meteorological data collected on-site or at a nearby weather station (Fletcher et al., 2021). Several equations are presented in the literature to estimate ET, with the most common being FAO-56 Penman–Monteith (Allen et al., 1998). Guo et al. (2016) presents 21 different methods for determining ET from meteorological data, with some methods being more suitable depending on data availability. This manuscript will adopt the ET naming conventions of FAO-56 Penman–Monteith presented in Allen et al. (1998).

A limitation of many ET estimation techniques is the assumption of 'perfect' well-watered conditions for a reference crop, e.g. a mono-culture of short-cropped grass for reference ET ($ET_o$) in FAO-56 Penman–Monteith. In practice, vegetation water use strategies and soil water availability heavily influence the actual ET rates that occur within vegetated SuDS (Berretta et al., 2014; Poë et al., 2015). $ET_o$ values can be factored to account for a variety of vegetation types through the application of a crop coefficients ($K_c$) (Berretta et al., 2014; Szota et al., 2017; Jahanfar et al., 2018; Hess et al., 2019). $ET_o$ can also be scaled to account for varying soil moisture conditions (water stress) by applying a water stress coefficient ($K_s$) or a soil moisture extraction function (SMEF), for which Zhao et al. (2013) present numerous formulations.

Values of actual ET can therefore be calculated via:

$$ET = K_c \times ET_o \times f(\theta, \theta_{fc}) \quad (1)$$

where $f(\theta, \theta_{fc})$ represents the SMEF as a function of soil moisture content, $\theta$, and soil field capacity, $\theta_{fc}$.

### 1.4. Physical measurements of ET and $K_c$

Physical measurements of ET are necessary to develop robust $K_c$ values and understand the volumetric stormwater retention performance of vegetated SuDS. The literature presents numerous methods for determining ET, which range in spatial scale from a single leaf (Porometry, Askari et al., 2021) up to entire bioretention systems (Lysimetry, Green et al., 2021). Fletcher et al. (2021) provide a comprehensive overview of these methods.

A lysimeter, a device that measures actual plant–soil evapotranspiration from a bounded soil volume, is amongst the simplest and most accurate of methods for the physical determination of ET. Lysimeters can be constructed at a variety of spatial scales and typically operate as either drainage (Berretta et al., 2014; Green et al., 2021) or weighing (Poë et al., 2015; Hess et al., 2017) lysimeters, where water volumes or system masses are measured respectively. However, weighing lysimeters are not generally practical for field-scale systems (Fletcher et al., 2021).

Several studies have successfully used lysimetry to identify ET rates in pilot-scale green roofs (Wadzuk et al., 2013; Berretta et al., 2014; Poë et al., 2015; Szota et al., 2017; Jahanfar et al., 2018), bioretention systems (Muthanna et al., 2008; Hess et al., 2017; Green et al., 2021) and tree-pits (Szota et al., 2018). However, lysimetry alone only provides bulk estimates of soil moisture. The incorporation of moisture content sensors within the bounded soil volume of the lysimeter can provide greater insight into moisture gradients with depth (Berretta et al., 2014; Green et al., 2021; Hess et al., 2021). These insights, coupled with vegetation rooting depth knowledge, allow a better understanding of how ET rates may change due to soil moisture content (and hence plant available water).

Relatively little research has focused on the identification of crop factors specifically for typical SuDS vegetation types or planting mixes. Berretta et al. (2014), Starry et al. (2016), Szota et al. (2017) and Jahanfar et al. (2018) determined values of $K_c$ from direct observations of moisture loss in green roofs. Starry et al. (2016) also noted several earlier studies on green roof systems which have reported crop factors ranging from 0.52 to 3.25. In a similar study to that of Berretta et al. (2014), Starry et al. (2016) used reference ET and moisture content data from green roof platforms – after having adjusted for water stress – to identify crop coefficients for three different species of common green roof succulents. The mean value of $K_c$ determined

[2] 'Soil moisture' is a term from the Soil Science field, upon which much SuDS process knowledge is built. The 'soil' within SuDS most commonly refers to the growing media. However, it should be noted that many SuDS growing media mixes have very different physical characteristics compared with natural soils (De-Ville et al., 2021). Unless clearly stated, the terms 'soil' and 'growing media' should be assumed to be analogous in this article.

over a full calendar year was 0.38, with seasonal and species-specific differences noted. In contrast, based on glasshouse experiments with well-watered specimens, Soni et al. (2022) suggested $K_c$ values that were considerably higher, ranging from 1.9–2.2 and 2.7–3.8 for green roofs with shallower and deeper substrates respectively.

Fewer researchers have focused on bioretention cells. Hess et al. (2019) derived $K_c$ values for a single bioretention vegetation mix consisting of three species common to bioretention systems in Pennsylvania, USA. Their work provides insight into the seasonal fluctuations of $K_c$, with values of 0.3 to 2.0 found for Spring and Summer, respectively. Ouédraogo et al. (2022) used eight 1 $m^3$ weighing lysimeters over three years to study ET rates in urban raingardens in Paris, France. ET rates were found to be higher than reference ET values, but not particularly sensitive to vegetation type.

The lack of consensus to date on suitable $K_c$ values to employ within modelling and design tools for bioretention cells is a clear motivation for the current research.

### 1.5. Significance of ET for stormwater management

Supplementary Material S1 summarises a number of key recent studies focusing on the water balance of various vegetated SuDS devices. At the device scale, ET from bioretention systems typically accounts for 3%–16% of the water balance (10th and 90th percentiles, respectively, of 18 systems across 8 studies). This low proportion reflects the concentrated inflows to these systems, where catchment area to device area ratios can be as high as 25:1 (Woods Ballard et al., 2015). In contrast, green roofs conventionally only handle incident rainfall, and ET typically accounts for > 50% of the water balance. It is important to note that, in several of the bioretention studies, ET values were estimated by closing the water balance based on inflow, outflow and water table observations, due to the difficulties involved in accurately monitoring ET in the field.

For the 18 bioretention studies considered in Supplementary Material S1, exfiltration is the predominant mechanism by which stormwater volumes are reduced, accounting on average for 36.6% of the water balance. However, in unfavourable ground conditions (low infiltration rates), ET losses can be similar in magnitude to exfiltration losses (Delvecchio et al., 2019). In highly developed urban areas, exfiltration is not always possible due to unsuitable ground conditions, pollutant risks, or a need to protect existing buried infrastructure. In these conditions, bioretention systems are often lined, and ET becomes the only process by which system retention capacities can be recovered between rainfall events.

The current evidence base suggests that ET volumes from bioretention systems may be low compared with losses due to exfiltration. These findings, alongside the complexities of predicting ET, may result in the volumetric reduction capabilities of ET being ignored during the design process, leading to oversized bioretention designs (Spraakman et al., 2022).

For ET to be properly accounted for in the SuDS design process, engineers require robust modelling tools that accurately capture the way in which the system's actual ET rates vary as a function of climatic inputs ($ET_o$), vegetation treatment and growth stage, and moisture availability. This paper presents new data from continuously monitored controlled laboratory column lysimeter tests intended to support the development and application of appropriate modelling and design tools. Column lysimeters have specific advantages in this context, in particular their ability to yield continuous time-series of ET data. The same lysimeters were also used in a runoff detention study, which is not discussed here. The Discussion section to the present paper provides some reflections on the limitations of the chosen methodology, including suggestions for further work.

### 1.6. Aim & objectives

This study aims to quantify evapotranspiration from three common bioretention vegetation treatments. This aim will be achieved via the following objectives:

- Establish a set of bioretention lysimeters that can be subjected to controlled and continuous evapotranspiration assessment.
- Observe the evapotranspiration behaviour of three common bioretention vegetation treatments compared with an unvegetated control through repeated experiments in different seasons and plant growth stages, and subject to moisture stressed conditions.
- Explore the suitability of moisture content measurements for evapotranspiration assessment.
- Determine appropriate vegetation treatment-specific crop coefficients and SMEF models to allow actual ET to be identified from $ET_o$.
- Define the significance of observed evapotranspiration rates on the stormwater performance of a representative field-scale bioretention system via a continuous hydrological model.

## 2. Materials & methods

### 2.1. Bioretention column specification

A set of 12 cylindrical Bioretention Columns was constructed to replicate the complete depth profile of pilot-scale bioretention lysimeters located at the UK Collaboratorium for Research on Infrastructure and Cities (UKCRIC) National Green Infrastructure Facility (NGIF), Newcastle-upon-Tyne, UK (see Green et al., 2021). Columns were numbered from 1 to 12 and are herein referred to as C1 to C12. Each column was 152 mm in internal diameter and 1100 mm tall and comprised (from bottom to top): a 180 mm drainage layer of 4/40 mm aggregate, a 120 mm transition layer of 2/6 mm aggregate, a 700 mm layer of growing media, and a 100 mm ponding zone (Fig. 2a). A 16 mm diameter outlet valve was installed near the base of each column to permit saturation or drainage of the columns, as required.

The growing media for this study was sourced locally within Sheffield, UK, and comprised 100% recycled waste components. The waste components were (by weight): 50% Quarry Waste Material (5–20 mm); 25% Crushed Recycled Glass; 15% Green Waste Compost; and 10% Sugar-beet Washings (topsoil). The physical characteristics of this media are presented fully in De-Ville et al. (2021). The media has a saturated hydraulic conductivity of 101 mm/h, porosity of 0.443 $m^3/m^3$, and field capacity of 0.149 $m^3/m^3$. Field capacity is at the lower end of the range of values reported in the literature; this is likely due to the higher than usual gravel content. The media is 43.7% fines and sand, and 56.3% gravel. The growing media is used extensively throughout Sheffield in the City Council's Grey-to-Green retrofit bioretention systems (Susdrain, 2016).

Four vegetation treatments were trialled (in triplicate) across the 12 columns. These were: an un-vegetated control (C1–C3), an Amenity Grass mix (C4–C6), and mono-cultures of a tufted hair-grass (C7–C9, *Deschampsia cespitosa* 'Goldtau') and an iris (C10–C12, *Iris sibirica* 'Ruffled Velvet,' Fig. 2c). All four vegetation treatments were established in September 2020. The Amenity Grass mix was grown from seed, while the *D. cespitosa* and *I. sibirica* were transplanted from 2 litre pots. The columns were maintained and allowed to establish over the winter of 2020–21 ahead of the first climate chamber trials in April 2021. Between climate chamber trials (May 2021–September 2021, October 2021–April 2022), the columns were located outdoors and were subject to regular irrigation and weeding. The *D. cespitosa* and *I. sibirica* were both cut back at the end of each winter period in accordance with local bioretention vegetation maintenance recommendations.

The Amenity Grass was kept to an approximate height of 120 mm in line with FAO-56 Penman–Monteith guidance for a reference surface

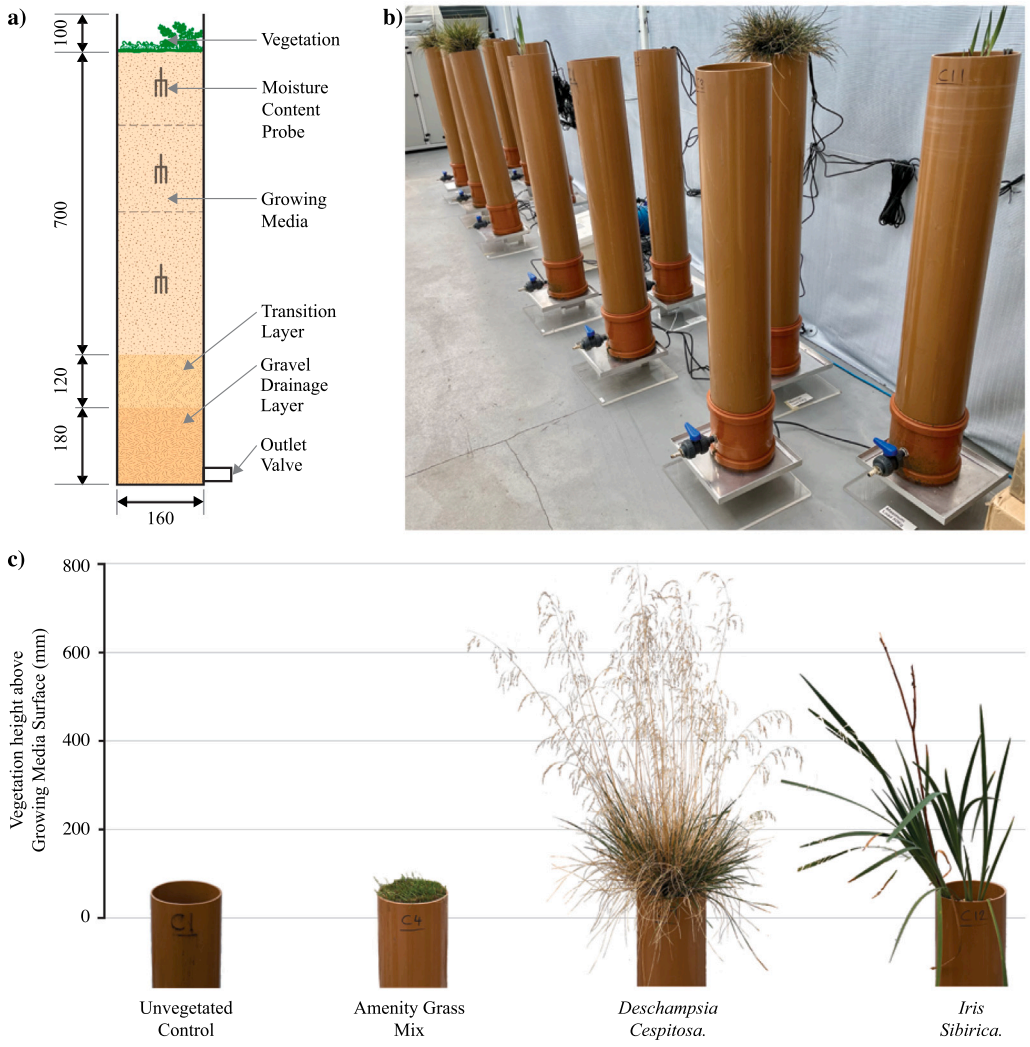


**Fig. 2.** The Bioretention Columns: (a) Schematic cross-section that indicates moisture probe locations (where installed) and soil volumes associated with each probe. All dimensions in mm. (b) Assembled columns on load cells inside the growth chamber (April 2021). (c) Examples of the four vegetation treatments (September 2021).

to enable its suitability as a reference crop to be evaluated alongside its performance as a representative bioretention vegetation treatment. It should be noted that this treatment has two potential limitations as a reference crop: (i) the use of a narrow column rather than an extensive homogeneous field; and (ii) the deliberate introduction of water stress.

### 2.2. Climate control facilities

Observations took place within a climate-regulated greenhouse exposed to ambient lighting conditions at The University of Sheffield's Arthur Willis Environment Centre (Sheffield, UK). The climate in the United Kingdom is defined as a humid temperate oceanic climate, or Cfb on the Köppen–Geiger climate classification system. Temperature and relative humidity were controlled within the growth chamber, while solar radiation levels were restricted (via semi-transparent blinds) only when extreme sunlight levels affected temperature control performance. Meteorological variables used in the determination of FAO-56 Penman–Monteith $ET_o$ were monitored at a 30 s temporal resolution using a central CR1000X data-logger (Campbell Scientific); a summary of these variables is provided in Table 1. Net radiation estimates were sourced from a CNR4 Net Radiometer located 1.42 km from the growth chamber positioned above a green roof with Sedum vegetation. Given the constant rate of air exchange into and out of the climate chamber, a wind speed survey was conducted after the testing period at 0.2 m above the column surfaces using a TSI Airflow TA410 air velocity meter, and this data set was assumed to represent conditions across all trials. The mean wind speed from this survey (120 samples, $\overline{u} = 0.673$ m/s) was then scaled to a wind speed at the standard 2 m elevation ($u_2 = 1.56$ m/s) using Equation 47 from Allen et al. (1998).

**Table 1**
Summary of sensors used for data acquisition.

| Variable | Sensor | Accuracy | Precision |
|---|---|---|---|
| Mass | 50 kg Load Cell | ±0.30 g | 0.075 g |
| Volumetric Water Content | 5TM (Dielectric Permittivity) | ±1 [-] | 0.1 [-] |
| Air Temperature | HygroVUE10 | ±0.2 °C | 0.001 °C |
| Relative Humidity | HygroVUE10 | ±1.5% | 0.01% |
| Net Radiation | CNR4 | – | 0.01 W/m$^2$ |

### 2.3. Climate conditions

Five 14-day trials were conducted across three distinct data collection periods: April–May 2021, September–October 2021, and April–May 2022. These are henceforth referred to as Trial I–V. The target conditions within the growth chamber during each of these five trials are presented in Table 2. Climate conditions were varied throughout

**Table 2**
Summary of trial target conditions.

| Trial | Season | Day Temp. (°C) | Night Temp. (°C) | Relative humidity (%) | No. of 14-day observations |
|---|---|---|---|---|---|
| I | Spring | 18.5 | 15.0 | 70 | 1 |
| II, III | Summer | 22.5 | 18.5 | 70 | 2 |
| IV, V | Spring | 18.5 | 18.5 | 70 | 2 |

the trials in an attempt to replicate typical mid-Spring (April–May) and late Summer (September) diurnal variations based on historical climate data for Sheffield, UK (De-Ville et al., 2020). In Trials IV and V, the diurnal temperature cycle was removed to eliminate complications related to the temperature-dependent behaviour of the load cells.

### 2.4. Test procedure

Each column was placed on its respective load cell inside the climate-regulated growth chamber. The outlet control valves were closed and water was applied until a ponding depth of at least 50 mm was achieved to saturate the columns. The columns were left in a saturated state for 24 h before the outlet control valves were opened for a period of 2 h. After the 2-hour drain-down period, the outlet control valves were closed and the columns were left for 14 days without irrigation or maintenance. At the end of the 14-day dry period, columns were irrigated and maintained where necessary. For the paired consecutive trials (Trials II–III and IV–V), the columns were left for a 48-hour period before the above process was repeated for a second time. After the second 14-day period, the columns were again irrigated and maintained before being returned to the outdoor growth location.

### 2.5. Evapotranspiration monitoring

#### 2.5.1. Continuous mass evaluations

To continuously evaluate ET via mass loss, the 12 columns were each placed onto their own load cell (Fig. 2b). Once the outlet valve was closed for the duration of each trial, the only pathway for mass loss was the return of water to the atmosphere via ET. Each load cell had a 50 kg capacity (RLS050, RDPE) and was connected to the central CR1000X data-logger with mass measurements taken at 30 s intervals. Load cell precision and accuracy are detailed in Table 1. Load cells were calibrated prior to each climate chamber trial. Calibrations were not found to change significantly over the 18-month duration of the experimental programme. However, during the course of the experimental programme, a temperature dependency in the load cell output was identified. A temperature correction was developed and implemented to mitigate this behaviour (see De-Ville and Stovin, 2023).

Values of mass loss, $\Delta M$ (kg), were converted to observed mass loss ET estimates, $ET_{\Delta M}$ (m), via:

$$ET_{\Delta M} = -\frac{4 \times \Delta M}{\rho_w \times \pi \times D^2} \tag{2}$$

where $\rho_w$ is the density of water (assumed constant at 1000 kg/m$^3$) and $D$ is the column diameter in m (i.e 0.152 m).

#### 2.5.2. Continuous moisture evaluations

To continuously evaluate ET via growing media moisture content, a vertical array of moisture content probes (METER 5TM) was installed during column construction. Six of the twelve columns contained a moisture content probe array: a single unvegetated column (C2), all three Amenity Grass columns (C4–C6), a single *D. cespitosa* column (C8) and a single *I. sibirica* column (C11). The moisture content probes were positioned vertically at depths of 100, 300 and 500 mm below the growing media surface (Fig. 2a). Each moisture content probe was connected to the CR1000X data-logger and moisture content was recorded at 30 s intervals as dielectric permittivity. A media-specific lab-derived calibration equation was used to convert from dielectric permittivity to volumetric water content (see De-Ville and Stovin, 2023). Moisture content sensor precision and accuracy are detailed in Table 1.

Values of moisture loss, $\Delta\theta$ (m$^3$/m$^3$), were converted to observed moisture loss ET estimates, $ET_{\Delta\theta}$ (m), via:

$$ET_{\Delta\theta} = -\sum_{1}^{n} (\Delta\theta_n \times Z_n) \tag{3}$$

where $n$ is the number of moisture zones (volumes attributed to a specific change in moisture content, $\Delta\theta_n$) and $Z_n$ is the vertical depth of the moisture zone (m). For this study, columns were divided into three moisture zones centred around each probe of the vertical moisture content sensor array. The uppermost zones were 0.2 m deep, while the lower zone was 0.3 m deep (Fig. 2a). Together, these zones covered the full 0.7 m depth of growing media.

### 2.6. Reference ET temporal profiles

Two estimates of reference evapotranspiration were considered at an hourly resolution for each trial:

- $ET_o$ was calculated using collected meteorological data and the FAO-56 Penman–Monteith method (Equation 53 from Allen et al., 1998).
- $ET_c$ was estimated from the Amenity Grass experimental columns at hourly time steps ($t$) using mass loss and moisture content data:

$$ET_{c,t} = \frac{1}{N}\sum_{i=1}^{N}\left(\frac{ET_{\Delta M,i,t}}{f_G(\theta_{bulk,i}, \theta_{fc})_t}\right) \tag{4}$$

where $N$ is the number of columns ($N = 3$ in Trial I and $N = 2$ in Trials II–V due to sensor failure) and $f_G$ is the Amenity Grass specific SMEF. $ET_c$ represents the ET that would have occurred from the reference crop, had moisture been unrestricted throughout the tests.

Eq. (5) provides the most basic form of SMEF:

$$f(\theta_{bulk}, \theta_{fc}) = \left(\frac{\theta_{bulk}}{\theta_{fc}}\right) \tag{5}$$

where $\theta_{bulk}$ is the weighted mean moisture content of the growing media, and $\theta_{fc}$ is the growing media's moisture content at field capacity ($\theta_{fc} = 0.15$, defined at a matric potential of 10 kPa, De-Ville et al., 2021). Supplementary Material S2 details how best-fit SMEF equations were identified for each of the three vegetation treatments. Zhao et al. (2013) identified multiple different forms of SMEF, and it is interesting to note that a different form of SMEF equation was required for each of the three vegetation treatments considered here.

### 2.7. Determination of crop coefficients

Crop coefficients for each vegetated column in each trial were determined using Eq. (1), where ET was the hourly observations of $ET_{\Delta M}$, $ET_o$ was derived from monitored climate variables, and $f(\theta_{bulk}, \theta_{fc})$ was calculated from soil moisture observations. Values of the unknown parameter, $K_c$, were determined via the least squares method. The model fit statistic $R^2$ (Nash and Sutcliffe, 1970) was used to evaluate the goodness-of-fit between observed $ET_{\Delta M}$ and values for actual ET estimated using the identified $K_c$ for each trial.

This process was repeated with $ET_c$ used in place of $ET_o$ as the reference ET to identify $K_{c,R}$ and $K_{c,P}$ respectively. Note that the requirement for moisture content data means that only the $K_c$ estimates for Amenity Grass were replicated ($N = 2$ due to sensor failure).

### 2.8. Statistical analyses

Non-parametric inferential statistical tests (Kruskal–Wallis and Dunn's pairwise comparisons) were conducted to identify any statistical independence between grouped data at the .05 significance level ($\alpha$). These tests were only conducted on the total cumulative ET derived from the mass-loss data ($N = 3$); the moisture loss and crop coefficient data lacked sufficient replication for statistical analysis. Caution should be exercised when interpreting the exact $P$ values derived from these statistical tests given the low sample sizes of this study.

### 2.9. Continuous hydrological modelling

The impacts of crop coefficient values on the ET proportion of the annual water balance were evaluated using the hydrological modelling framework proposed in Berretta et al. (2018). By tracking growing media moisture content, the model generates a continuous hourly estimate of ET and system outflow for a representative bioretention cell in each 12 km grid square of the British Isles. This data was used to estimate the corresponding ET contribution to the annual water balance by dividing total ET by total system inflow.

The physical configuration of the modelled bioretention system was set to replicate the pilot-scale bioretention lysimeters located at NGIF, as detailed in De-Ville et al. (2021). A simple scenario was considered in which inflows from a 20 $m^2$ catchment (e.g. a portion of road surface) were directed to a 2 $m^2$ bioretention cell (10:1 loading ratio) with an instantaneous time of concentration. The modelled cell was considered to be lined (no exfiltration) and incorporated an unrestricted underdrain outlet, which conveyed any runoff generated to a receiving sewer/watercourse. As the annual water balance is strongly influenced by local climatic controls, the intention was to explore how local climate, combined with different crop factors, would impact the annual water budget. Hourly rainfall and $ET_o$ data were sourced from the UK Climate Projections 2018 Regional Climate Model for the entire UK and Ireland at a spatial resolution of 12 km and corresponding to the 10-year period from 2020 to 2030 (Met Office Hadley Centre, 2018; Robinson et al., 2021).

## 3. Results

Fig. 3 presents the complete data record for Trial I (April–May 2021). Fig. 3a presents the meteorological data at an hourly resolution, and diurnal cycles are clearly visible in all variables. Fig. 3b presents the cumulative ET derived from the mass loss ($ET_{\Delta M}$) and moisture loss ($ET_{\Delta\theta}$) methods. For the mass loss data, each data point represents a mean value from three replicate columns, with the surrounding shaded region indicating the observed range across replicates. Fig. 3c presents the ET data from three specific 48-hour periods during the early (day 3–4), mid (day 8–9), and late (day 13–14) periods of each trial. This highlights any trends in ET resulting from the continuous loss in soil moisture during each trial. Daily values of $ET_o$ are also included.

The data presented in Fig. 3 corresponds to one of the five trials completed in this study. Analogous figures corresponding to the other four trials are available in Supplementary Material S3, and the underlying data is available in De-Ville and Stovin (2023). The following sections present the full data set in depth, focusing particularly on the effects of vegetation treatment and soil moisture restrictions.

### 3.1. Reference evapotranspiration estimates ($ET_o$)

Table 3 summarises the observed meteorological variables from within the chamber during each trial, alongside the externally sourced net radiation data, and the resultant $ET_o$ values. Air temperatures within the growth chamber exhibited variations from the target values for each trial (Table 2), with up to a 4.1 °C exceedance during Trial I (Day 6, Fig. 3). Substantial deviations from target values of relative

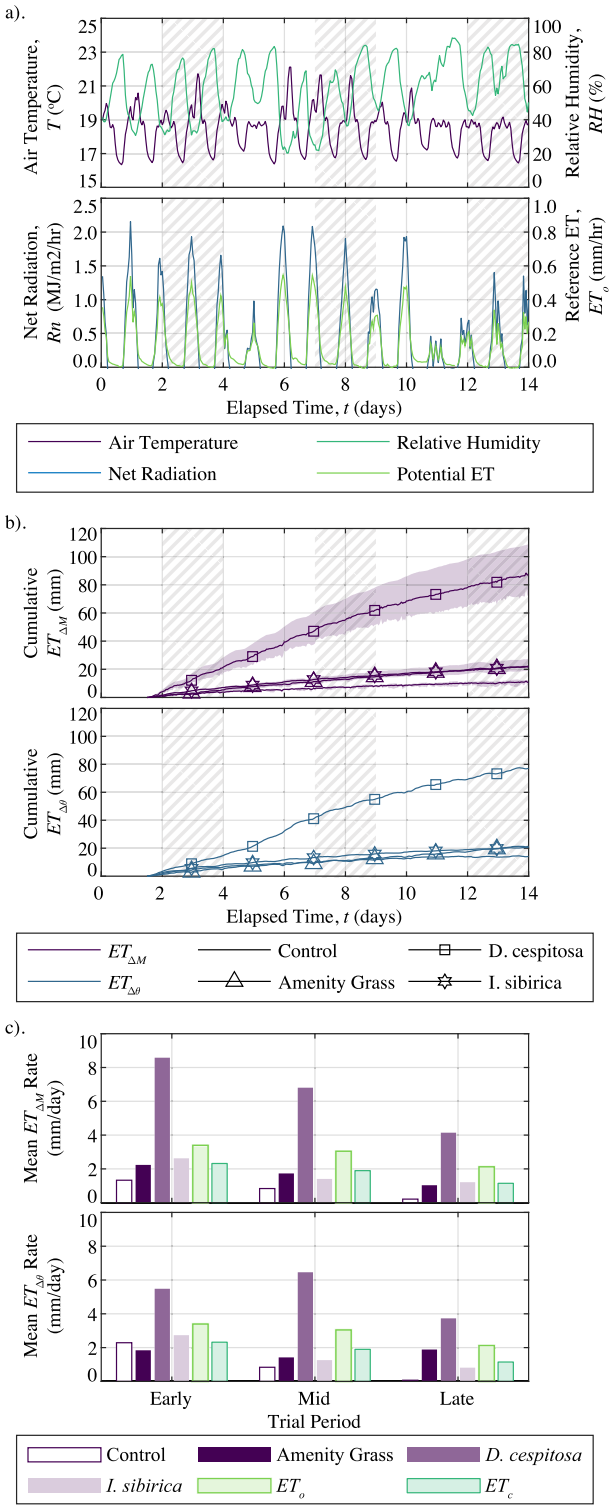


**Fig. 3.** Complete data record for Trial I. (a). Collected meteorological data. (b). Cumulative ET derived from the mass loss ($ET_{\Delta M}$) and moisture loss ($ET_{\Delta\theta}$) methods, shaded regions represent range of observed values. (c). Comparison of $ET_{\Delta M}$ and $ET_{\Delta\theta}$ with reference predictions ($ET_o$ and $ET_c$) in the early (day 3–4), mid (day 8–9) and late (day 13–14) period of the trial [vertical hatched regions in (a). and (b).].

**Table 3**
Summary statistics of observed meteorological variables.

| Trial | | I | II | III | IV | V |
|---|---|---|---|---|---|---|
| Air Temperature (°C) | Min. | 16.3 | 18.3 | 18.2 | 17.0 | 17.6 |
| | Mean | 18.5 | 21.2 | 21.1 | 17.9 | 18.2 |
| | Max. | 22.6 | 22.8 | 23.0 | 19.6 | 19.6 |
| Relative Humidity (%) | Min. | 20.2 | 42.6 | 36.7 | 27.9 | 31.0 |
| | Mean | 58.3 | 77.1 | 75.1 | 44.6 | 46.5 |
| | Max. | 88.5 | 91.6 | 92.5 | 64.4 | 62.5 |
| Net Radiation (MJ/m$^2$) | Total | 108.5 | 66.8 | 65.1 | 181.5 | 141.5 |
| $ET_o$ (mm/day) | Min. | 1.6 | 1.2 | 0.6 | 2.4 | 2.4 |
| | Mean | 3.0 | 1.9 | 2.0 | 4.2 | 3.6 |
| | Max. | 4.7 | 2.8 | 3.3 | 6.0 | 5.6 |

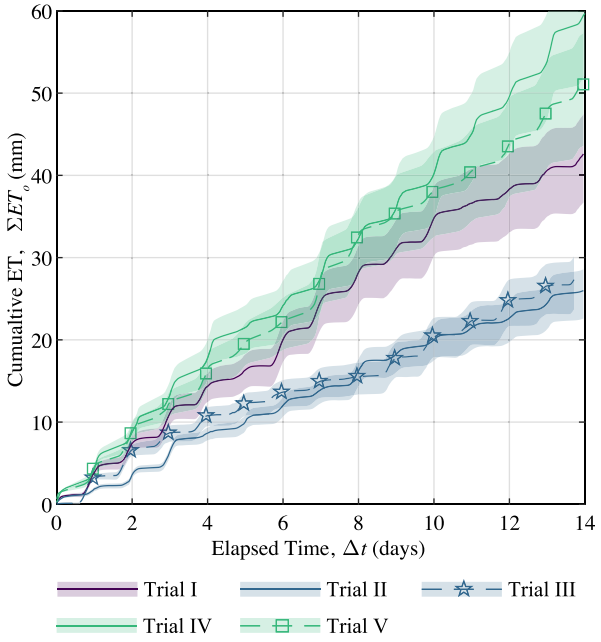


**Fig. 4.** Cumulative $ET_o$ across the five trials. Shaded regions indicate propagated range of uncertainty from sensor accuracy.

humidity (i.e. 70%) were also observed, with lows of 20.2% and highs of 92.5%. These deviations can be attributed to external humidity fluctuations and the mechanical limitations of the climate control system allowing only modest control of relative humidity.

Net radiation – and consequently $ET_o$ values – were lowest during Trials II and III (Table 3), despite these taking place during the (calendar) Summer of 2021 (Table 2 and Fig. 4). Similarly, the lower relative humidity conditions of 2022 Spring Trials (IV and V) were also more conducive to elevated $ET_o$ rates. The calculated values of $ET_o$ are comparable to values typically observed in Sheffield, UK, where mean values range from 2.3 mm/day in Spring to 3.2 mm/day in Summer (2016–2020 long-term averages, Environment Agency, 2021). However, the actual climatic conditions observed during the trials are clearly not representative of typical or expected Spring/Summer differences; for this reason analysis of data by season is not included in the subsequent analysis.

An analysis of observed meteorological variable sensor errors (Table 1) was conducted, and the effects of these errors on cumulative $ET_o$ prediction were quantified (Fig. 4). Over the 14-day trial periods, these errors were at most ±7.6 mm (Trial IV), which represents a 12.7% error.

### 3.2. Mass-loss evapotranspiration estimates

Fig. 5 presents mass-loss derived cumulative ET ($\Sigma ET_{\Delta M}$) data for an example column from each vegetation treatment for each of the five trials. The unvegetated column, C2, exhibited high levels of consistency in cumulative ET data across the five trial-periods, showing little sensitivity to the varying climate conditions (Table 3). Similar behaviour was seen in all three of the control columns (Supplementary Material S4) and is reinforced via a Kruskal–Wallis test which identified no statistical independence between the total cumulative ET of the three unvegetated columns across the five trials ($N = 3, P = .112, \alpha = .05$, Fig. 6a).

With respect to differences observed between the trials as a result of plant age or season, it should be recalled that the actual weather conditions experienced during the trials did not reflect typical Spring/Summer differences. In the vegetated columns (C4, C8 and C11), the greatest cumulative ET was typically observed in Trials IV–V, which coincided with elevated $ET_o$ (Fig. 6a, Table 3). However, *D. cespitosa* columns exhibited the greatest cumulative ET during Trial I (Spring of 2021) before falling by more than 60% in Trials II–III (Summer of 2021). The results from Trial I and Trial III for this treatment were found to be statistically independent ($N = 3, P = .022, \alpha = .05$). The Amenity Grass columns only exhibited statistical independence between Trial I and Trial V ($N = 3, P = .012, \alpha = .05$). These isolated results, and a lack of any statistical independence in cumulative ET for *I. sibirica* columns across the five trials ($N = 3, P = .212, \alpha = .05$), suggest that no systematic 'seasonal' or plant age variations in cumulative ET were observed.

Given the above findings, grouping of the data by trial was removed to assess the differences observed between vegetation treatments. Fig. 6b highlights the statistical independence ($N = 15, P = .000, \alpha = .05$) in cumulative ET between the unvegetated and vegetated columns of any treatment, i.e. vegetated columns exhibited greater ET than unvegetated columns. However, it also highlights that there was no statistical independence between the cumulative ET of any of the vegetated treatments.

### 3.3. Moisture-loss evapotranspiration estimates

Moisture loss data from the top 100 mm of growing media for the unvegetated control, Amenity Grass and *I. sibirica* columns are presented in Fig. 7. As with the mass-loss data, there was a high degree of consistency in the observed moisture loss over time within the unvegetated control columns, confirming the repeatability of the experimental method. Fig. 8 presents the moisture loss data across the full depth of the *D. cespitosa* column, where significant moisture content reductions were observed at greater depths. The full profiles for all columns are available in Supplementary Material S5.

The moisture loss profiles for all columns at all depths were characterised by a steep initial gradient which reduced over time (Figs. 7 and 8). This phenomenon is a result of continuing percolation within the column after the control valve has been closed. After approximately 1.5 days, moisture loss gradients became shallower and more closely reflect losses due to ET alone. Nasrollahpour et al. (2022) also observed gravity drainage periods of around 1.5 days before ET processes were the dominant driver of moisture loss in bioretention mesocosms of a similar depth to the bioretention columns of this study. Data from the first 1.5 days of each trial period were therefore excluded from subsequent analysis.

The moisture loss data corroborates the mass-loss findings, with the Amenity Grass and *I. sibirica* columns exhibiting greater moisture loss than the unvegetated control for Trial I (Fig. 7). The moisture loss data across the full depth of the *D. cespitosa* column in Trial I shows evidence of root moisture scavenging from increasing depth over time (Fig. 8). On day 6, the moisture at 100 mm depth had fallen by 15%, and the gradient of the moisture loss at a depth of 300 mm began to increase around the same time, indicating accelerating moisture loss from this region. On day 10, the moisture at a depth of 300 mm had fallen by almost 15% and a corresponding increase in moisture loss gradient can

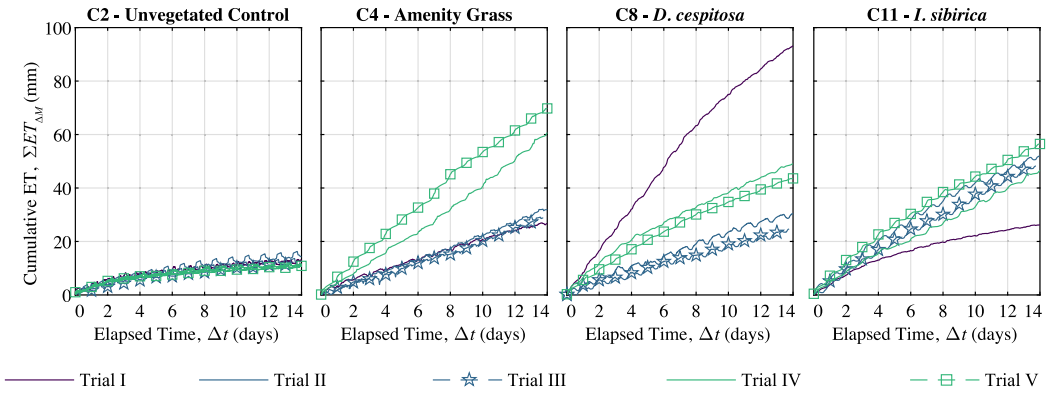


**Fig. 5.** Cumulative ET derived from observed Mass-loss data. One example column from each vegetation treatment. Associated climate conditions are presented in Table 3.

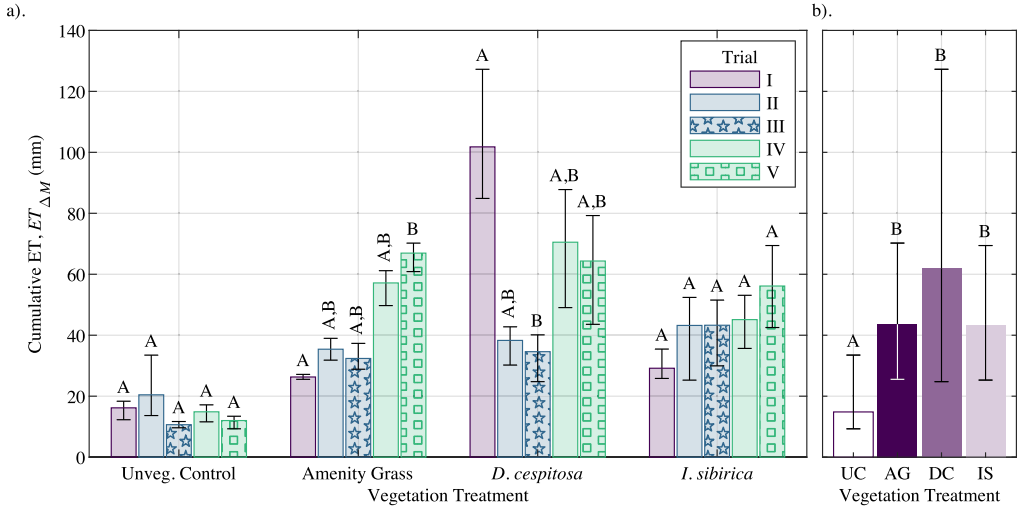


**Fig. 6.** Statistical analyses of mass-loss derived ET data ($ET_{\Delta M}$). (a). Mean cumulative ET for each vegetation treatment across the five trials ($N$ = 3). Error bars indicate the range of observations. Statistical groupings within each vegetation treatment are shown by capital letters above each bar. (b). Mean cumulative ET for each vegetation treatment combined across the five trials ($N$ = 15). Error bars indicate the range of observations. Statistical groupings are shown by capital letters above each bar.

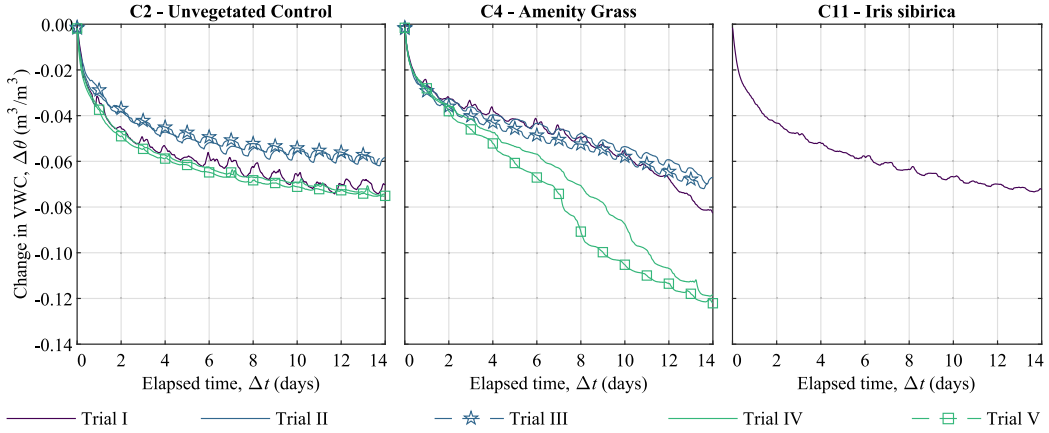


**Fig. 7.** Moisture loss data at 100 mm depth for the unvegetated control, Amenity Grass and *I. sibirica* columns. Moisture data is not available for *I. sibirica* from Trials B and C due to sensor failure.

be seen at a depth of 500 mm as deep roots began to extract water in the lower region of the column.

The above results, and the recent findings of Hess et al. (2021) and Nasrollahpour et al. (2022), confirm that soil moisture content monitoring is an effective way of determining ET in lab- or pilot-scale bioretention systems.

### 3.4. ET vs. $ET_o$

Comparisons of ET, derived from the mass loss ($ET_{\Delta M}$) and moisture loss ($ET_{\Delta\theta}$) methods, with the two reference ET estimates ($ET_o$ and $ET_c$) were conducted from day 1.5 onwards. The data for Trial V are presented in Fig. 9 (all trial results are presented in Supplementary Material S6). Good agreement was noted between $ET_{\Delta M}$ and $ET_{\Delta\theta}$ for

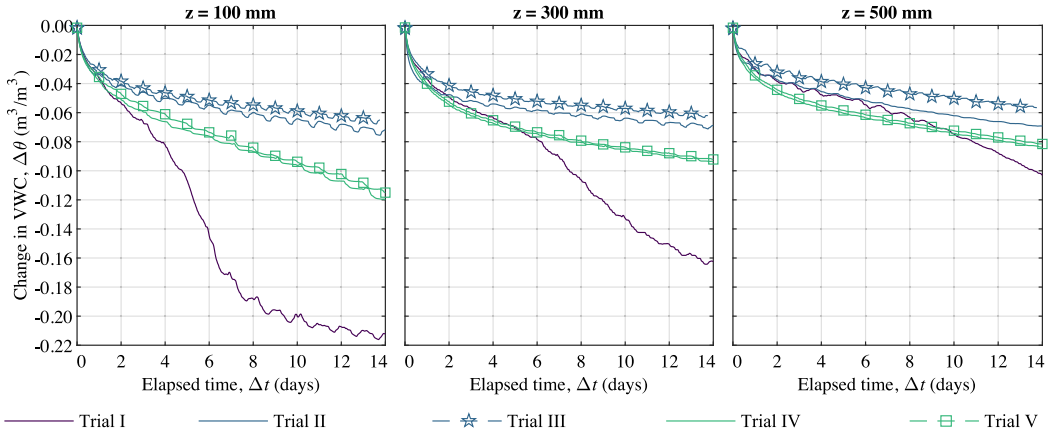


**Fig. 8.** Moisture loss data across the full depth of the *D. cespitosa* column (C8).

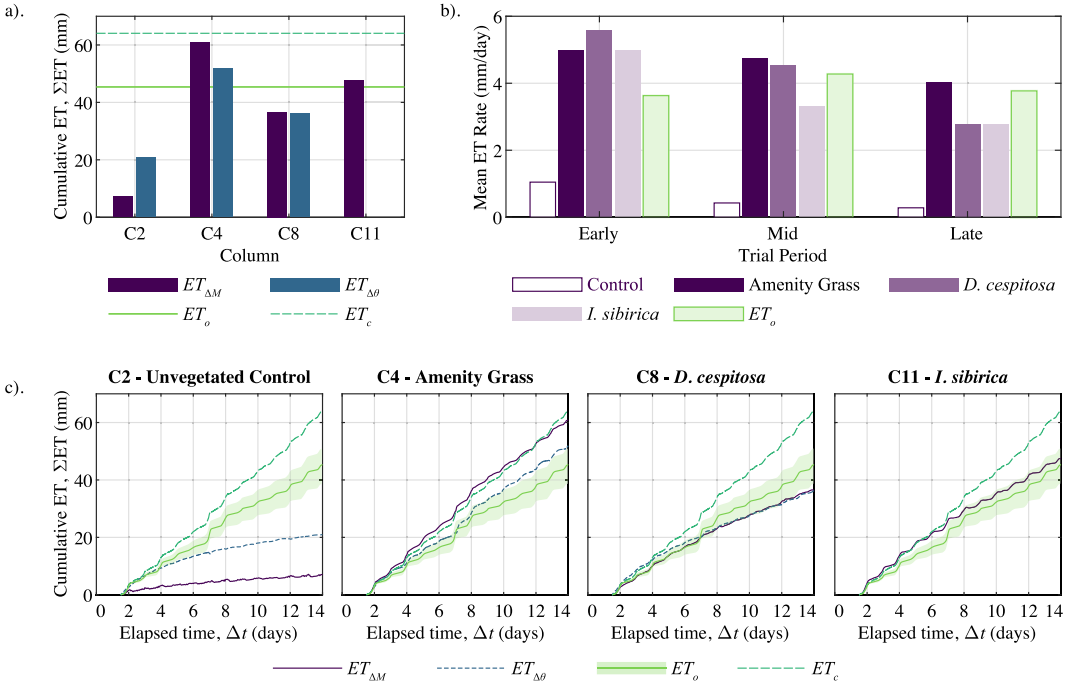


**Fig. 9.** Trial V ET Comparisons from day 1.5 to 14. (a). Summary comparison of ET derived from Mass-loss ($ET_{\Delta M}$) and Moisture-loss ($ET_{\Delta\theta}$) methods with reference ET predictions ($ET_o$ and $ET_c$). (b). Comparison of $ET_{\Delta M}$ and $ET_o$ in the early (day 3–4), mid (day 8–9) and late (day 13–14) period of the trial. (c.) Cumulative $ET_{\Delta M}$ and $ET_{\Delta\theta}$ compared with $ET_o$ and $ET_c$.

the vegetated columns (Fig. 9a), although cumulative $ET_{\Delta\theta}$ at the end of each trial was typically below cumulative $ET_{\Delta M}$ (Supplementary Material S6). This is due to the 1.5 day cutoff used to account for observed percolation; the exact time for ET to have become the dominant mechanism of moisture removal will vary for each column.

When comparing $ET_{\Delta M}$ with $ET_o$, consistent trends were observed between the four column configurations. In the unvegetated control column (C2) $ET_o$ estimates exceeded $ET_{\Delta M}$ (Fig. 9a). This behaviour is expected given the lack of transpiration contribution towards ET in this column configuration. For vegetated configurations, there is no clear pattern in the comparison between $ET_o$ and $ET_{\Delta M}$. Amenity Grass columns (C4) typically exhibited higher $ET_{\Delta M}$ than $ET_o$, *D. cespitosa* (C8) typically exhibited lower $ET_{\Delta M}$ than $ET_o$, while the *I. sibirica* (C11) $ET_{\Delta M}$ changes from below $ET_o$ to above $ET_o$ during Trials IV–V, replicating behaviour seen across all trials (Supplementary Material S6). This variation reflects the different ET performance of each species and their continuing establishment throughout the experimental programme.

Daily ET rates derived from $ET_{\Delta M}$ for all column configurations exhibited a clear reduction in ET over the duration of each Trial (Fig. 9b). This reduction occurred despite the relatively constant rate of $ET_o$ (approximately 4 mm/day) and is due to reductions in soil moisture content which become the controlling factor on ET performance during each trial. Despite similar initial ET rates, the Amenity Grass exhibited a smaller reduction in ET rate over time compared with either *D. cespitosa* or *I. sibirica*. This observation reinforces the need for treatment-specific SMEF relationships.

The dynamics of observed ET were generally consistent with $ET_o$. In Trial V, the peak net radiation occurring on day 7 resulted in increased $ET_o$, manifested as a visible 'step' in the cumulative $ET_o$ profile (Fig. 9c). A corresponding 'step' is seen in the $ET_{\Delta M}$ profiles of both the Amenity Grass and *I. sibirica* columns.

The $ET_c$ values—derived from $ET_{\Delta M}$ and $\theta_{bulk}$ data for Amenity Grass columns (C4–6)—unsurprisingly show good agreement with the Amenity Grass column (C4, Fig. 9c). Note that cumulative measured ET for C4 was lower than the $ET_c$ estimate derived from the same data

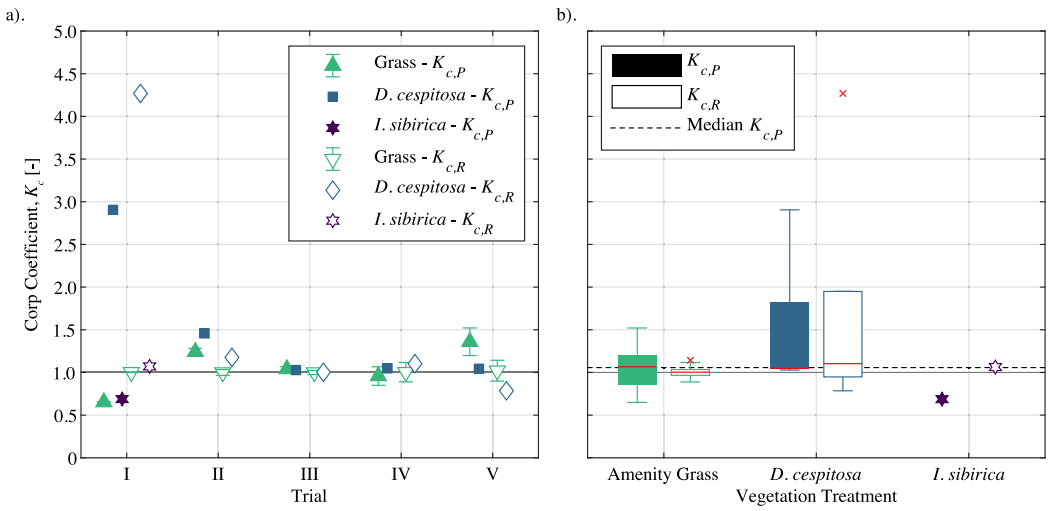


**Fig. 10.** Crop coefficients $K_{c,P}$ and $K_{c,R}$. (a). $K_c$ values for all trials. Marker locations indicate median value, error bars indicate minimum and maximum values where $N > 1$. (b). Boxplot of all study $K_c$ values by vegetation treatment. Red horizontal lines indicate median values, boxes indicate interquartile range, whiskers indicate range of data, outliers are indicated by red × and are identified by being 1.5× the interquartile range lower/higher than the lower/upper quartile.

because the $ET_c$ estimate was corrected for soil moisture restrictions. $ET_c$ was considerably higher than $ET_o$ for Trial V and Trial II. However, this behaviour was not consistent, as Trial I exhibited lower $ET_c$ than $ET_o$ (Supplementary Material S6). This variable relationship between $ET_c$ and $ET_o$ suggests that the ET behaviour of the Amenity Grass columns is not stable between trials and, as such, does not fully meet reference crop standards.

### 3.5. Crop coefficients

The optimised crop coefficients for the vegetation treatments ($K_{c,P}$ and $K_{c,R}$, derived from $ET_o$ and $ET_c$ data respectively) are presented in Fig. 10. Individual crop coefficients for each column during each trial, and their associated model fit statistics, are presented in Supplementary Material S7. Values of $K_{c,P}$ ranged from 0.65 to 2.91 and $K_{c,R}$ from 0.79 to 4.27.

Amenity Grass column crop coefficients determined using $ET_o$ ($K_{c,P}$) were not consistent across all trials, ranging from 0.65 to 1.36 (Fig. 10a), due to the aforementioned non-compliance with reference crop standards. However, Amenity Grass column crop coefficients determined using $ET_c$ were consistent at $K_{c,R} = 1.0$ (Fig. 10a). This was anticipated, as values of $ET_c$ were determined by assuming these columns represented a reference short-cropped grass (Eq. (4)). There is some variation between the three replicates of the Amenity Grass columns, as demonstrated by the range bars in Fig. 10a, arising from subtle differences in substrate and vegetation characteristics.

For *D. cespitosa* columns, the identified crop coefficients for Trial I were up to 4× higher than all other values ($K_{c,R} = 4.27$). These crop coefficients reflect the high values of both $ET_{\Delta M}$ and $ET_{\Delta\theta}$ for *D. cespitosa* in Trial I. From Trial III onwards, values of $K_{c,P}$ did not exceed 1.05. The $K_{c,P}$ values of the Amenity Grass and *D. cespitosa* columns did not exhibit any visually observable systematic differences between trials (Fig. 10a).

Given observations of no statistical independence in total ET between trials (Section 3.2), values of $K_c$ have been combined across all trials to permit statistical analysis (Fig. 10b). For $K_{c,P}$ values, no statistical independence was identified between the Amenity Grass ($N = 10$, Median $K_{c,P} = 1.07$) and *D. cespitosa* ($N = 5$, Median $K_{c,P} = 1.05$) columns ($P = .462, \alpha = .05$). A similar outcome was observed for $K_{c,R}$ values ($P = .327, \alpha = .05$). Crop coefficients for *I. sibirica* are only available for Trial I (due to moisture content sensor failure), hence they could not be included in this analysis.

With the exception of Trial I values, where vegetation is hypothesised to have still been establishing, crop coefficients identified using $ET_o$ as the reference ET were approximately equal to 1.0 (Median $K_{c,P} = 1.06$, Fig. 10b). Seasonal differences between Trials II–III (Summer) and Trials IV–V (Spring) were absent within the identified crop coefficients. The findings of this study suggest that, in the absence of a fuller understanding of system dynamics, a constant crop coefficient of 1.0 would be a pragmatic, and conservative, default value for modelling actual ET in vegetated SuDS.

### 3.6. Modelled hydrological impact

The experimental findings of this study identified unique soil moisture extraction function (SMEF) formulations for each vegetated column configuration. A SMEF is required as part of any continuous simulation model to account for the reductions in actual ET that occur when the growing media moisture content falls below field capacity. However, it was noted that the additional complexity of the alternative models offered trivial improvement in model fit statistics compared with the most straightforward SMEF formulation (Supplementary Material S2). Hence, the most straightforward SMEF formulation (Eq. (5)) was utilised within the continuous hydrological model and the authors recommend it be used as a default approach for modelling actual ET in SuDS.

Integration of the SMEF alongside the determined crop coefficients within a long-term continuous simulation hydrological model demonstrates the typical ET proportion of a 10-year water balance and the effect crop coefficients can have on the volumes of stormwater returned to the atmosphere. Fig. 11 presents the projected rainfall and $ET_o$ that was used to calculate a 10-year water balance for the British Isles. Fig. 12 presents the water balance proportion data for the lowest and highest observed $ET_o$ derived crop coefficients ($K_c = 0.65$, $K_c = 2.91$) alongside the proposed default value of 1.0 across the British Isles for the period 2020 to 2030. Areas of high rainfall (northwest Scotland) correlate with areas of low $ET_o$ as a result of increased cloud cover and coincident reduced solar radiation, while the inverse is true around the Thames estuary and along the south coast of England (Fig. 11). Hence, the resultant ET proportion of the water balance closely resembles the $ET_o$ distribution, with stronger performance (higher losses due to ET) in the southeast of England and weaker performance in northwest Scotland (Fig. 12). The application of a crop coefficient of 2.91 results in approximately 4.5× the volume of water being returned to the atmosphere (14.4%, spatial median) when compared to a crop coefficient of 0.65 (3.2%) and 2.9× the volume for a crop coefficient of 1.0 (5.0%).

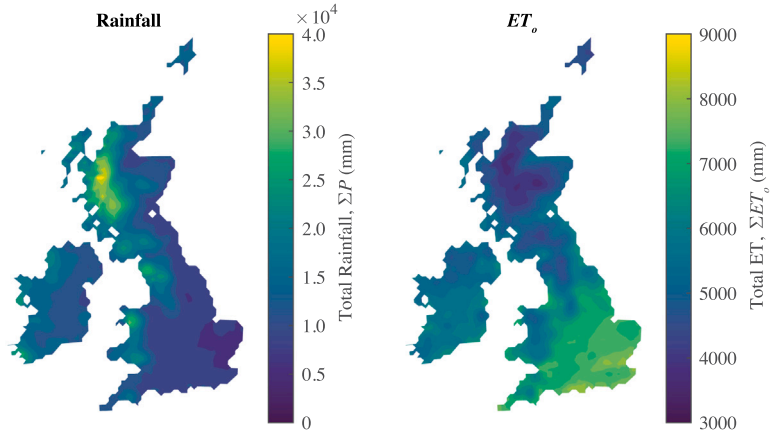


**Fig. 11.** Bioretention hydrological model inputs. 10-year UKCP18 rainfall and $ET_o$ data from 2020 to 2030 across the British Isles.

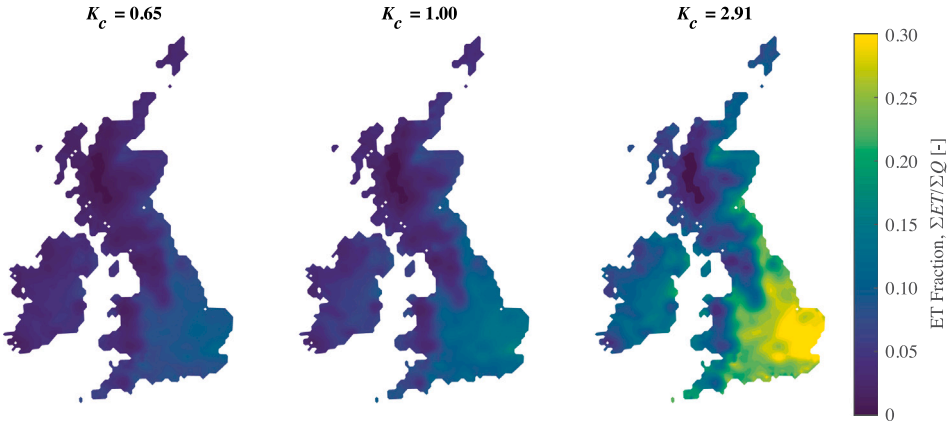


**Fig. 12.** Bioretention hydrological model outputs. ET proportion of the 10-year water balance at varying values of Crop Coefficient ($K_c$) across the British Isles.

## 4. Discussion

### 4.1. Influence of vegetation treatment, water stress, season and growth stage

Detailed observations over five 14-day trials showed that all treatments had a consistent response to moisture stress, which can be represented in hydrological models via a SMEF. Total cumulative ET of vegetated and non-vegetated columns were identified to be statistically independent, with vegetated columns returning greater volumes of water to the atmosphere. In some vegetation treatments, the mass-loss derived ET in Trial I was statistically independent from later trials, suggesting that those treatments may not have been fully established at the time of Trial I. While insufficient replicates containing moisture content probes were available to support statistical analysis of the derived crop coefficients across trials, the data presented in Fig. 10a also suggests that systematic differences as a result of vegetation treatment or plant age were not evident once the plants were fully established.

Seasonal differences were expected (Allen et al., 1998), but not consistently observed. This is in contrast to the findings of Hess et al. (2019), where three distinct crop coefficients were identified over the course of an annual growing cycle. Additional crop coefficients were identified by Hess et al. (2019) to account for varying bioretention lysimeter configuration (growing media and drainage outlet) for a consistent vegetation mix. The lack of seasonal variation in the present study reflects the occurrence of uncharacteristic weather patterns such that Spring conditions were unusually hot and dry and Summer conditions were cooler than typically observed.

### 4.2. Methodological limitations

While the column lysimeters of this study have provided valuable insights into ET losses from different bioretention vegetation treatments, certain limitations have to be acknowledged. In the study, losses were reported with respect to the plan area of the column and not to the projected area of the plants, which varied noticeably between treatments (see Fig. 2). In a similar study, Soni et al. (2022) acknowledged that high ET rates measured in potted green roof/bioretention plants might reflect the fact that their leaves extended well outside the pot area. Bioretention planting in practice typically involves heterogeneous plant mixes at a fixed planting density (e.g. 9 plants per $m^2$) irrespective of an individual plant's expected final dimensions. Therefore the combined data from our individual treatments may be considered to be reasonably indicative of the combined effects of different plants/treatments. However, data from plants monitored in isolation may also overestimate their *in situ* ET, as sheltering by other plants in the canopy is not considered.

Additional risks associated with the use of column tests in this context are due to edge effects, which may lead to more pronounced heating/cooling of the soil column than would be experienced in the ground, and also lead to preferential pathways for soil moisture. For the unvegetated control, as noted by Soni et al. (2022), the raised edges of the column/pot may have contributed some shading and wind sheltering effects, leading to reduced evaporation.

This study used a controlled environment growth chamber to ensure dry periods in excess of 14 days, something which is not necessarily achievable outdoors during typical UK Spring or Summer conditions. However, this introduced additional uncertainties into the methodology that raise further questions about the transferability of identified

crop coefficients to external environments. For example, attempts were made to quantify solar radiation within the growth chamber. Observations of total shortwave radiation and net radiation followed the dynamics of values observed at an externally located net-radiometer (Section 2), but they had approximately one-third the magnitude. The exact mechanism by which net-radiation within the chamber appears reduced compared to an external environment – but results in typical levels of plant transpiration – cannot be identified from the collected data. Further discussion of evaluating ET in a climate controlled environment can be found in Supplementary Material S9.

The extent to which any laboratory determination of ET rates or crop factors can fully represent an installed system in the field is inherently limited. Heterogeneous vegetation mixes, urban micro-climates, urban heat island fragmentation and wind-canyon effects further complicate the determination of urban ET when using estimation methods designed for agricultural use. The integration of multiple different crop factors to account for plant types, growth stages, growing media, bioretention cell physical configuration and micro-climatic setting is unlikely to ever be considered practical for engineering application in the field, an acknowledgement which further supports the authors' pragmatic recommendation that a crop factor of 1.0 should be adopted for modelling and design purposes.

We recommend that further research efforts place greater focus on attempting to quantify ET from real bioretention cells with typically heterogeneous vegetation mixes, potentially exploiting some of the remote sensing techniques that are already well-established in agricultural moisture balance work (Qiu et al., 2021).

### 4.3. Implications of the current study for bioretention cell design and modelling

It is important to be conscious that bioretention systems are not source control interventions (Woods Ballard et al., 2015). They are designed to control runoff from a much larger catchment compared to their surface area (the area available for ET). Hence, their potential for volumetric stormwater reductions – particularly in the lined systems of the modelling exercise – is lower than, for example, green roofs or permeable pavements. The hydrological model output for the British Isles has identified that there is significant spatial variation in the contribution that ET makes to the annual water balance of a generic lined bioretention system (Fig. 12). When focusing on the $K_c = 1.0$ scenario, as recommended herein, ET is shown to account for between 1% (Northwest Scotland) and 12% (Thames Estuary) of the water balance across the British Isles. These values are comparable with the range of observed ET contributions to the water balance in the literature, irrespective of differences in system physical configuration, loading ratio, or climatic setting. Loading ratios would need to be reduced in wetter locations to achieve the higher ET contributions noted in drier locations.

The output of the continuous hydrological model permits a more detailed interrogation of ET dynamics (and hence bioretention system retention performance) on a rainfall event-by-event basis (Supplementary Material S8). ET leads to a soil moisture deficit, which equates to the device's retention capacity. For a small rainfall event, this soil moisture deficit may lead to 100% retention. However, the proportional retention losses associated with high return period design storms tend to zero, and should generally be ignored in bioretention design. By acknowledging the limited volumetric losses associated with ET in bioretention systems, stormwater planners can provide landscape architects with more agency to maximise the amenity and ecological benefits of bioretention planting schemes.

## 5. Conclusions

This study assessed the significance of evapotranspiration (ET) and the complexity of predicting actual ET in bioretention systems. ET estimates were derived from the mass and moisture loss data of three vegetation treatments commonly found in UK bioretention systems (Amenity Grass, *Deschampsia cespitosa* and *Iris sibirica*). A total of 840 column days of ET data was collected from 12 columns across five trials, each of 14 days in length. These estimates of ET were compared with predictions made using observed meteorological variables and the FAO-56 Penman–Monteith $ET_o$. Crop coefficients were determined for the three vegetation treatments and used within a long-term continuous hydrological model to demonstrate the volumetric reduction potential of a generic bioretention system across the British Isles.

This study has determined that:

- ET rates of the three tested vegetation treatments varied, although in most cases the differences were not statistically independent. The most significant deviations from $ET_o$ arose during the first trial when the vegetation was still establishing.
- ET rates derived from moisture content data were comparable with mass loss-derived estimates once ET became the dominant flux over percolation.
- Reduced rates of ET were associated with reduced moisture availability which necessitates the use of a soil moisture extraction function to estimate actual evapotranspiration.
- Optimised crop coefficients for each treatment were within the range of crop coefficients reported elsewhere in the literature for bioretention systems.
- Without scenario-specific empirical data, a crop coefficient of 1.0 is a sensible initial estimate for evaluating ET in vegetated SuDS.
- Application of the optimised crop coefficients within a long-term continuous hydrological model of a bioretention system with a loading ratio of 10:1 highlighted that volumetric reductions associated with ET are dependent upon climatic and rainfall conditions but can be expected to account for 1%–12% of the annual water balance.

## Declaration of competing interest

The authors declare that they have no known competing financial interests or personal relationships that could have appeared to influence the work reported in this paper.

## Data availability

The processed laboratory data at an hourly resolution from the five trial periods are available via The University of Sheffield's Online Research Data Archive (De-Ville and Stovin, 2023). Raw data may be made available upon request via the corresponding author.

## Acknowledgements

This research was funded by the United Kingdom's Engineering and Physical Sciences Research Council (EPSRC) grant numbers EP/S005536/1 and EP/S005862/1.

## Appendix A. Supplementary data

Supplementary material related to this article can be found online at https://doi.org/10.1016/j.watres.2024.121182.

## References


Allen, R.G., Pereira, L.S., Raes, D., Smith, M., 1998. Crop evapotranspiration-guidelines for computing crop water requirements-FAO irrigation and drainage paper 56. FAO, Rome 300 (9).

Askari, S.H., De-Ville, S., Hathway, E.A., Stovin, V., 2021. Estimating evapotranspiration from commonly occurring urban plant species using porometry and canopy stomatal conductance. Water 2021, Vol. 13, Page 2262 13 (16), 2262. http://dx.doi.org/10.3390/W13162262.

Berretta, C., Aiello, A., Jensen, H.S., Tillotson, M.R., Boxall, A., Stovin, V., 2018. Influence of design and media amendments on the performance of stormwater biofilters. Proc. Inst. Civ. Eng. - Water Manag. 171 (2), 87–98. http://dx.doi.org/10.1680/jwama.16.00121.

Berretta, C., Poë, S., Stovin, V., 2014. Moisture content behaviour in extensive green roofs during dry periods: The influence of vegetation and substrate characteristics. J. Hydrol. 511, 374–386. http://dx.doi.org/10.1016/J.JHYDROL.2014.01.036.

Blyth, E.M., Martínez-de la Torre, A., Robinson, E.L., 2019. Trends in evapotranspiration and its drivers in great britain: 1961 to 2015. Prog. Phys. Geogr. 43 (5), 666–693. http://dx.doi.org/10.1177/0309133319841891.

Butler, D., Digman, C.J., Makropoulos, C., Davies, J.W., 2018. Urban drainage, 4ed. Urban Drainage, fourth ed. Taylor & Francis Group, p. 587.

De-Ville, S., Green, D., Edmondson, J., Stirling, R., Dawson, R., Stovin, V., 2021. Evaluating the potential hydrological performance of a bioretention media with 100% recycled waste components. Water 2021, Vol. 13, Page 2014 13 (15), 2014. http://dx.doi.org/10.3390/W13152014.

De-Ville, S., Stovin, V., 2023. Urban Green DaMS: Evapotranspiration in Bioretention Systems Data. The University of Sheffield, http://dx.doi.org/10.15131/shef.data.21641306.

De-Ville, S., Stovin, V., Berretta, C., Werdin, J., Poë, S., 2020. Hadfield Green Roof 5-year dataset. http://dx.doi.org/10.15131/shef.data.11876736.v1.

Delvecchio, T., Welker, A., Asce, M., Wadzuk, B.M., Asce, A.M., 2019. Exploration of volume reduction via infiltration and evapotranspiration for different soil types in rain garden lysimeters. J. Sustain. Water Built Environ. 6 (1), 04019008. http://dx.doi.org/10.1061/JSWBAY.0000894.

Environment Agency, 2021. Environment Agency Potential Evapotranspiration Dataset. data.gov.uk, URL https://www.data.gov.uk/dataset/7b58506c-620d-433c-afce-d5d93ef7e01e/environment-agency-potential-evapotranspiration-dataset#licence-info.

Fletcher, T.D., Bertrand-Krajewski, J.-L., Bonneau, J., Burns, M.J., Poelsma, P.J., Thom, J.K., 2021. Measuring the water balance in stormwater control measures. In: Bertrand-Krajewski, J.-L., Clemens, F., Lepot, M. (Eds.), Metrology in Urban Drainage and Stormwater Management: Plug and Pray. IWA Publishing, London, pp. 105–134. http://dx.doi.org/10.2166/9781789060119.

Fletcher, T.D., Shuster, W., Hunt, W.F., Ashley, R., Butler, D., Arthur, S., Trowsdale, S., Barraud, S., Semadeni-Davies, A., Bertrand-Krajewski, J.L., Mikkelsen, P.S., Rivard, G., Uhl, M., Dagenais, D., Viklander, M., 2014. SUDS, LID, BMPs, WSUD and more – The evolution and application of terminology surrounding urban drainage. Urban Water J. 12 (7), 525–542. http://dx.doi.org/10.1080/1573062X.2014.916314.

Green, D., Stirling, R., De-Ville, S., Stovin, V., Dawson, R., 2021. Investigating bioretention cell performance: A large-scale lysimeter study. In: EGU General Assembly. Vienna, Austria, p. online. http://dx.doi.org/10.5194/EGUSPHERE-EGU21-10259.

Guo, D., Westra, S., Maier, H.R., 2016. An R package for modelling actual, potential and reference evapotranspiration. Environ. Model. Softw. 78, 216–224. http://dx.doi.org/10.1016/J.ENVSOFT.2015.12.019.

Hess, A., Asce, M., Wadzuk, B., Welker, A., 2017. Evapotranspiration in rain gardens using weighing lysimeters. J. Irrig. Drain. Eng. 143 (6), 04017004. http://dx.doi.org/10.1061/(ASCE)IR.1943-4774.0001157.

Hess, A., Wadzuk, B., Welker, A., 2021. Evapotranspiration estimation in rain gardens using soil moisture sensors. Vadose Zone J. 20 (1), e20100. http://dx.doi.org/10.1002/VZJ2.20100.

Hess, A.J., Wadzuk, B.M., Welker, A., Hess, A., Asce, M., Wadzuk, B., 2019. Predictive evapotranspiration equations in rain gardens. J. Irrig. Drain. Eng. 145 (7), http://dx.doi.org/10.1061/(ASCE)IR.1943-4774.0001389.

Jahanfar, A., Drake, J., Sleep, B., Gharabaghi, B., 2018. A modified FAO evapotranspiration model for refined water budget analysis for Green Roof systems. Ecol. Eng. 119, 45–53. http://dx.doi.org/10.1016/J.ECOLENG.2018.04.021.

Met Office Hadley Centre, 2018. UKCP18 Regional Projections on a 12km Grid Over the UK for 1980–2080. Centre for Environmental Data Analysis, URL https://catalogue.ceda.ac.uk/uuid/589211abeb844070a95d061c8cc7f604.

Muthanna, T.M., Viklander, M., Thorolfsson, S.T., 2008. Seasonal climatic effects on the hydrology of a rain garden. Hydrol. Process. 22 (11), 1640–1649. http://dx.doi.org/10.1002/HYP.6732.

Nash, J.E., Sutcliffe, J.V., 1970. River flow forecasting through conceptual models part I — A discussion of principles. J. Hydrol. 10 (3), 282–290. http://dx.doi.org/10.1016/0022-1694(70)90255-6.

Nasrollahpour, R., Skorobogatov, A., He, J., Valeo, C., Chu, A., van Duin, B., 2022. The impact of vegetation and media on evapotranspiration in bioretention systems. Urban For. Urban Green. 74, 127680. http://dx.doi.org/10.1016/J.UFUG.2022.127680.

Ouédraogo, A.A., Berthier, E., Durand, B., Gromaire, M.-C., 2022. Determinants of evapotranspiration in urban rain gardens: A case study with lysimeters under temperate climate. Hydrology 9 (3), http://dx.doi.org/10.3390/hydrology9030042, URL https://www.mdpi.com/2306-5338/9/3/42.

Poë, S., Stovin, V., Berretta, C., 2015. Parameters influencing the regeneration of a green roof's retention capacity via evapotranspiration. J. Hydrol. 523, 356–367. http://dx.doi.org/10.1016/J.JHYDROL.2015.02.002.

Qiu, G.Y., Wang, B., Li, T., Zhang, X., Zou, Z., Yan, C., 2021. Estimation of the transpiration of urban shrubs using the modified three-dimensional three-temperature model and infrared remote sensing. J. Hydrol. 594, http://dx.doi.org/10.1016/j.jhydrol.2020.125940.

Robinson, E., Kay, A., Brown, M., Chapman, R., Bell, V., Blyth, E.M., 2021. Potential Evapotranspiration Derived from the UK Climate Projections 2018 Regional Climate Model ensemble 1980–2080 (Hydro-PE UKCP18 RCM). NERC EDS Environmental Information Data Centre, http://dx.doi.org/10.5285/eb5d9dc4-13bb-44c7-9bf8-c5980fcf52a4.

Soni, L., Szota, C., Fletcher, T.D., Farrell, C., 2022. Influence of water storage and plant crop factor on green roof retention and plant drought stress. PLoS Water 1 (3), e0000009.

Spraakman, S., Martel, J.-L., Drake, J., 2022. How much water can bioretention retain, and where does it go? Blue-Green Syst. 4 (2), 89–107. http://dx.doi.org/10.2166/BGS.2022.002.

Starry, O., Lea-Cox, J., Ristvey, A., Cohan, S., 2016. Parameterizing a water-balance model for predicting stormwater runoff from green roofs. J. Hydrol. Eng. 21 (12), 04016046.

Susdrain, 2016. Grey to green phase 1, sheffield. URL https://www.susdrain.org/case-studies/case_studies/grey_green_phase_1_sheffield_light_case_study.html.

Szota, C., Farrell, C., Williams, N.S., Arndt, S.K., Fletcher, T.D., 2017. Drought-avoiding plants with low water use can achieve high rainfall retention without jeopardising survival on green roofs. Sci. Total Environ. 603–604, 340–351. http://dx.doi.org/10.1016/J.SCITOTENV.2017.06.061.

Szota, C., McCarthy, M.J., Sanders, G.J., Farrell, C., Fletcher, T.D., Arndt, S.K., Livesley, S.J., 2018. Tree water-use strategies to improve stormwater retention performance of biofiltration systems. Water Res. 144, 285–295. http://dx.doi.org/10.1016/J.WATRES.2018.07.044.

Wadzuk, B.M., Asce, M., Schneider, D., Feller, M., Traver, R.G., 2013. Evapotranspiration from a green-roof storm-water control measure. J. Irrig. Drain. Eng. 139 (12), 995–1003. http://dx.doi.org/10.1061/(ASCE)IR.1943-4774.0000643.

Woods Ballard, B., Wilson, Udale-Clarke, H., Illman, S., Scott, T., Ashley, R., Kellagher, R., 2015. The SuDS Manual C753. Technical Report, CIRIA, London.

Zhao, L., Xia, J., Xu, C.y., Wang, Z., Sobkowiak, L., Long, C., 2013. Evapotranspiration estimation methods in hydrological models. J. Geograph. Sci. 2013 23:2 23 (2), 359–369. http://dx.doi.org/10.1007/S11442-013-1015-9.